

Entropy-Driven Pumping in Zeolites and Biological Channels

Tom Chou^{1,*} and Detlef Lohse²

¹*Department of Physiology and DAMTP, Cambridge University, Cambridge CB3 9EW, England*

²*Department of Applied Physics and J. M. Burgers Centre for Fluid Mechanics, University of Twente, P.O. Box 217, 7500 AE Enschede, The Netherlands*

(Received 3 September 1998)

We simulate constrained dynamics of two species transport across single-file molecular-sized pores such as biomembrane channels and zeolites. We focus on diffusional pumping where one type of particle uses its entropy of mixing to drive another along its chemical potential gradient. Quantitative analyses of rates and efficiencies of transport are plotted as functions of transmembrane potential, pore length, and particle-pore interactions. Our results qualitatively explain recent measurements of “negative” osmosis and suggest new, more systematic experiments, particularly with zeolites. [S0031-9007(99)08931-0]

PACS numbers: 87.16.Dg, 05.60.-k, 66.30.Ny, 82.65.Fr

Particle transport across membranes is a crucial intermediate step in almost all biological and chemical engineering processes. Separation, catalysis, and drug release all rely on controlled transport through microscopic channels such as zeolites [1]. Biological examples include integral membrane proteins which traverse hydrophobic, highly impermeable lipid membranes and participate in small molecule transport [2].

When two binary solutions are separated by a permeable barrier, the individual species typically diffuse and mix, dissipating their chemical potential gradients. However, transport across both synthetic pores in mica sheets [3] and channels spanning biological membranes (e.g., gramicidin [4]) are known to exhibit constrained dynamics. For example, osmotically driven water flux [5] may be significantly reduced due to a counterflowing, permeable solute which couples to the solvent (water) within the confining pores [4,6,7]. We model these constrained dynamics with a one-dimensional lattice exclusion model. Specifically, we show that for large enough asymmetry between solvent-pore and solute-pore interactions, volume transfer can be in a direction *opposite* to that expected from simple osmosis. Here, one species of the otherwise counterflowing pair wins and forces the second to be coflowing. The efficiencies of this pumping mechanism are computed and found to be nonzero even when solutes are uncharged and not acted upon by direct, ponderomotive forces. Recent osmosis experiments in various systems [6,8,9] have indeed revealed negative reflection coefficients, i.e., volume flow opposite that expected from standard osmosis.

Since transmembrane pores such as gramicidin have typical radii $\sim 2\text{--}4$ Å, [4], and zeolites have typical radii $\sim 4\text{--}10$ Å, we use a one-dimensional exclusion model [10,11] to describe single-file particle flows. A single-file chain is divided into N sections labeled i , each of length $\ell \geq$ molecular diameters of A and B , and containing at most one particle of either type. The $A(B)$ occupation at site i is defined by $\tau_i, \tau'_i \in \{0, 1\}$. All parameters associated with $A(B)$ will carry unprimed (primed) notation.

The probability per unit time that an $A(B)$ particle enters from the left if site $i = 1$ is unoccupied is $\alpha\chi_L(\alpha'\chi'_L)$, where χ, χ' are the reservoir mole fractions of the particular types of particles that enter. Similarly, the entrance rates at $i = N$ are denoted by $\delta\chi_R(\delta'\chi'_R)$. We assume $\chi'_L = 1 - \chi_L > \chi'_R = 1 - \chi_R$ as depicted in Fig. 1(a). The $A(B)$ exit rates to the right (left) are denoted by β, γ and β', γ' . In the chain interior, A -type particles move to the right (left) with probability per unit time $p(q)$ *only* if the adjacent site is unoccupied. B particles hop left (right) under the same conditions with probability $p'(q')$.

Rigorous results exist for the two species asymmetric exclusion process under specific conditions [10]. However, currents for $N < 4$ can be easily found analytically

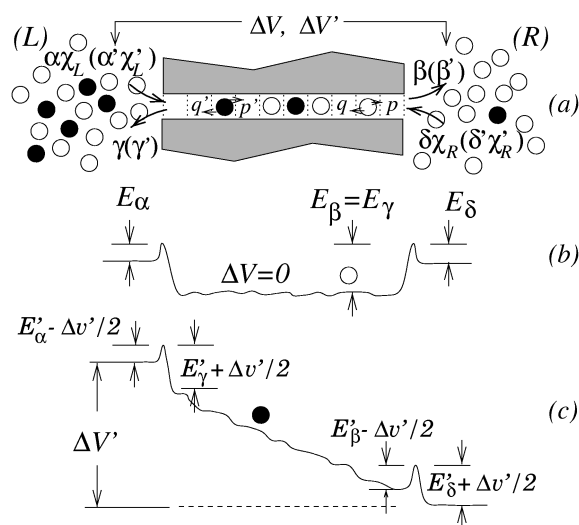


FIG. 1. (a) A two species 1D pore representing, e.g., zeolites or biological transport channels is divided into N sections of length ℓ . The kinetic rate constants for A (unprimed) and B (primed) particles are indicated. (b) and (c) depict energy barriers for A (open circles) and B (filled circles) particles. Assume A is uncharged ($\Delta V \equiv V_R - V_L = 0$), while B may be singly charged and acted upon by a transmembrane potential $\Delta V' \equiv V'_R - V'_L < 0$.

for general parameter sets by solving linear rate equations coupling all possible particle occupancy configurations [12]. For $N > 3$, lattice simulations describing the pore dynamics are implemented by choosing a site i and finding the instantaneous current between i and $i + 1$: $\hat{J}_i = \hat{p}\tau_i(1 - \tau_{i+1})(1 - \tau'_{i+1}) - \hat{q}\tau_{i+1}(1 - \tau_i)(1 - \tau'_i) \in \{0, \pm 1\}$, where $\hat{p} = 1$ with probability pdt , and zero with probability $(1 - p)dt$ as $dt \rightarrow 0$. Analogous expressions hold for the distribution of \hat{q} . The occupations τ_i, τ'_i are then updated and the next particle randomly chosen. An analogous rule holds for $\hat{J}'(\xi')$. Boundary site kinetics are correspondingly determined by $\alpha, \delta, \alpha', \delta'$, e.g., $\hat{J}_N = \hat{\beta}\tau_N - \hat{\delta}(1 - \tau_N)(1 - \tau'_N)$. Typically 10^{9-11} steps are needed for \hat{J}, \hat{J}' to converge to their steady state values, J and J' . We verified all results by comparing simulations with certain exact results [11,12].

Since particle fluxes across microscopic channels are $< 10^9/s$ [5,6], typical fluid particles suffer $> O(10^3)$ "collisions" and relax to local thermodynamic equilibrium (LTE) while traversing the pore. Under LTE, the kinetic rates, $\{\xi\} \equiv \{\alpha, \beta, \gamma, \delta, p, q\}$, can be estimated from Arrhenius forms

$$\begin{aligned} p &\approx q \approx (v_T/\ell) \exp(-E_p/k_B T), \\ \beta &\approx \gamma \approx (v_T/\ell) \exp(-E_\beta/k_B T), \\ \alpha, \delta &\approx \alpha_0 \exp(-E_\alpha/k_B T), \end{aligned} \quad (1)$$

with analogous expressions for $\{\xi'\} \equiv \{\alpha', \beta', \gamma', \delta', p', q'\}$. We have for simplicity assumed microscopically symmetric pores and equal hydrostatic pressures (i.e., $\beta = \gamma, \alpha = \delta$ and $\beta' = \gamma', \alpha' = \delta'$ when transmembrane potentials $\Delta V = 0$ and $\Delta V' = 0$, respectively) and also that within a narrow pore, particles equilibrate with the pore interior and relaxes momenta much faster than particle positions, implying, in the absence of external potentials, $p \approx q, p' \approx q'$. The hopping rates β, γ, p given in (1) represent ballistic travel times (thermal velocity v_T divided by section length), weighted by internal interaction energies E_p . The entrance energy dependent factors (α, δ) and (α', δ'), when multiplied by the relevant number fraction of entering particles, (χ_L, χ_R) and (χ'_L, χ'_R), respectively, define entrance rates into empty boundary sites. The precise values of the prefactors α_0, α'_0 will also depend on equilibrium parameters in the reservoirs such as temperature, total number density, and the effective area of the pore mouths. The energy barriers experienced during single particle transport are enumerated in Figs. 1(b) and 1(c) and may include external potentials. If say, the B particles have charge ze and are acted upon by a pondermotive transmembrane potential $\Delta V' \neq 0$, the energy barriers are shifted: $E'_{\alpha,\beta} \rightarrow E'_{\alpha,\beta} + k_B T v'/2$ and $E'_{\gamma,\delta} \rightarrow E'_{\gamma,\delta} - k_B T v'/2$, where $v' = ze\Delta V'/(N + 1)k_B T$. Thus, the kinetic rates when $v' \neq 0$ are

$$\begin{aligned} (\alpha', \beta', p') &\rightarrow (\alpha'_v, \beta'_v, p'_v) \equiv (\alpha', \beta', p') e^{-v'/2} \\ (\gamma', \delta', q') &\rightarrow (\gamma'_v, \delta'_v, q'_v) \equiv (\gamma', \delta', q') e^{+v'/2}. \end{aligned} \quad (2)$$

When $A(B)$ is uncharged (charged), J, J' are computed using the parameters $\{\xi\}, \{\xi'_v\} = (\alpha'_v, \beta'_v, \gamma'_v, \delta'_v, p'_v, q'_v)$, and $\chi'_{L,R}$.

Under isobaric, isothermal conditions, $\Delta E(P_L = P_R) = E_\alpha + E_\beta - E_\gamma - E_\delta = 0$, and since pressure fluctuations in liquid mixtures equilibrate much faster than concentration fluctuations, the total enthalpy change per $A(B)$ particle translocated is $\Delta H(\Delta H') \approx \Delta V(\Delta V')$. The efficiency of using species j to pump k can be defined as the ratio of the average free energy gained by k to the free energy lost by j ,

$$\eta_{jk} = [1 - \theta(J^j \Delta \mu^j)] \theta(J^k \Delta \mu^k) \frac{J^k(\chi'_{L,R}) \Delta \mu^k}{J^j(\chi'_{L,R}) \Delta \mu^j}. \quad (3)$$

The Heaviside functions represent the definition that flow is considered useful work only when j and k are coflowing. Using the entropy of mixing per particle $\Delta S' = k_B \ln(\chi'_L/\chi'_R)$, the Gibbs free energy change per particle, $\Delta \mu' = \Delta H' - T \Delta S'$, is

$$\Delta \mu' \approx k_B T \ln\left(\frac{\chi'_R}{\chi'_L}\right) + ze \Delta V', \quad (4)$$

with an analogous expression for $\Delta \mu$ associated with the transport of an A -type particle. When concentration differences are not too large, higher interaction terms contributing to $\Delta H, \Delta H'$ (and hence $\Delta \mu, \Delta \mu'$) can be neglected. These correction terms (which are higher order polynomials in $\Delta \chi, \Delta \chi'$) can be straightforwardly incorporated by independently measuring bulk liquid heats of mixing. For concreteness, we assume species $j = B$ (charged) is used to pump $k = A$ (uncharged) and that for liquids under ambient conditions $v_T/\ell \sim 1 \text{ ps}^{-1}$. Upon setting the time scale $dt = 10 \text{ fs}$, $p = q = p' = q' = 0.01 \ll 1$.

Figure 2 shows currents and efficiency as functions of a transmembrane potential difference $\Delta V' \neq 0$, for various length pores. Note that under the physiological conditions considered, the efficiencies are small ($\leq 1\%$) for pores of molecular lengths. A small $|\Delta \mu'|$ would increase efficiency via transpore energetics; however, for too large a $\Delta V'$, the B particles are driven back against their number gradient, and useful work precipitously vanishes. This occurs most easily for short channels where internal A - B interactions are rare; here $\Delta V' < 0$ is required for B to drive A uphill. The efficiency is nonmonotonic and has a maximum as $\Delta V'$ is varied for fixed $\{\xi, \xi'\}$ and $\chi'_{L,R}$.

For $ze\Delta V'/k_B T \rightarrow -\infty$, an asymptotic form for the efficiency can be found by assuming the B particles never hop against the potential gradient,

$$\eta(ze\Delta V'/k_B T \rightarrow -\infty) \sim \frac{\alpha e^{-|v'|}}{\alpha' N |v'|} \ln\left(\frac{1 - \chi'_R}{1 - \chi'_L}\right). \quad (5)$$

Although J' , which is dissipating down its electrochemical potential, generally decreases for longer pores, for small $\Delta V'$, $J(N = 10) > J(N = 5) > J(N = 3)$, because pumping is more efficient since there is less likelihood that a B particle can drift through without pushing out all the A particles ahead of it. The particle fluctuations

across the pore that allow A and B to simply dissipate their chemical potentials become rarer as membrane thickness or N increases, enhancing efficiency as shown in Fig. 3. Measurements for gramicidin channels suggest $N \sim 5-9$ [4,13]. Henceforth, unless otherwise indicated, we treat only entropic driving, i.e., $\Delta V = \Delta V' = 0$. Note that $\eta(N = 0, 1) = 0$ is exact for all parameters since $N = 0$ corresponds to an infinitely thin, noninteracting membrane, and an analytic solution for $J(N = 1) \propto \alpha\beta(\chi_R' - \chi_L')$ [11]. When $\Delta\mu > 0$, $\chi_R' < \chi_L'$ and $J < 0$, regardless of whether or not solute enters or passes through the single-site pore. This is expected since A and B never interact within the single-site pore for B to be able to “ratchet” A through. For larger N however, we find an asymptotic maximal efficiency defined by the kinetic parameters $\{\xi, \xi'\}$. As $N \rightarrow \infty$, the large fluctuations required for net particle transport will transfer a constant ratio of A and B particles. This asymptotic efficiency can be tuned by judiciously selecting $\{\xi, \xi'\}$ which yield the desired $N \rightarrow \infty$ performance. Note that for $ze\Delta V' = 0.3k_B T$, the $\eta(N \rightarrow \infty)$ limit is larger, but for short pores requires larger N both $J, J' > 0$ and pumping to take effect, consistent with the results in Fig. 2.

Performance can also be tuned by varying microscopic pore-molecule interactions. Recent simulations have demonstrated dynamic separation factors between species with different pore binding characteristics [14]. We suggest here that similar molecular considerations can be used to design pores [15] that operate as thermodynamic pumps, without moving parts, complex cooperative binding mechanisms [16,17], or external driving forces.

Figure 4 shows the effects of varying B -pore binding $\sim 1/\beta'$ for two different values of A -pore affinity α/β . Pores that do not strongly attract (larger β' [18]) or that

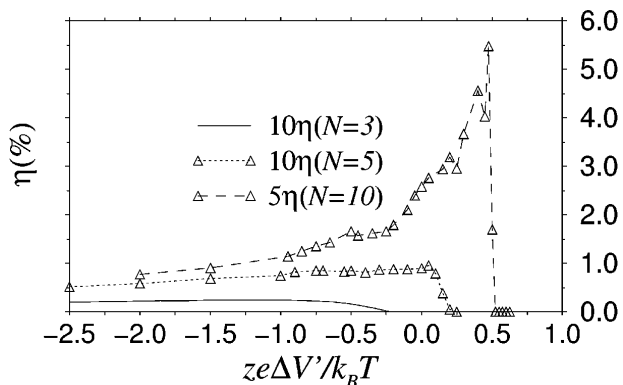


FIG. 2. $10\eta(N = 3)$ (exact, solid curves), $10\eta(N = 5)$, and $5\eta(N = 10)$ as functions of $\Delta V'$. The corresponding parameters (for a B -attracting pore) are $\beta = \gamma = p = p' = q = q' = 0.01$ ($dt = 10$ fs), and $\beta' = \gamma' = 0.003$. The intrinsic entrance rates here are $\alpha = \delta = \alpha' = \delta' = 0.01$. The smaller $\beta' < \beta, p, p'$ correspond to a pore that is more attractive to B than to A . Here, $\chi_L'/\chi_R' = (1 - \chi_L)/(1 - \chi_R) = 0.0036/0.0018$, corresponds to a 200 mM/100 mM aqueous B solution in $(L)/(R)$. The computed currents and efficiencies are low and (numerically) noisy due to low (physiological) concentrations χ' and entrance probabilities $\alpha'\chi'$.

repel solutes (smaller α') have lower B particle average occupations τ' , and allow solvent (A particles) to more likely pass from (R) to (L) , decreasing efficiency, consistent with recent osmosis experiments [8]. However, at very small β' (highly attracting pores), τ' increases to the point where it fouls the pore and decreases J relative to J' , also decreasing efficiency. Thus, there exists an intermediate B -pore affinity, which yields a maximum efficiency. Depending on A -pore affinity (dashed vs solid curves), currents and efficiencies can be simultaneously increased (e.g., by making pores slightly A repelling when $0.0028 \leq \beta' \leq 0.004$). These behaviors are a consequence of the intrinsic nonlinearities and are not present in the phenomenological linear Onsager limit [17].

The above results provide a microscopic theoretical framework for recent anomalous or “negative osmosis” experiments [8]. These measurements show negative osmosis only when the chemical structure of cation exchange membranes was modified by adding $-\text{CH}_2-$ functional groups. This modification presumably makes the pores smaller, enhancing the likelihood of finite particle size exclusion. More definitively, negative osmosis was measured within a window of fixed membrane charge ($-\text{CH}_2-\text{SO}_3^-$) density. Tuning these fixed counterion charges is equivalent to tuning β' for positively charged solutes (solute which exhibited anomalous osmosis were Ca^{+2} , Ba^{+2} , Sr^{+2} , and not H^+ , Na^+) [8]. Figure 4 shows a maximum in currents and pumping efficiency as a function of β' that qualitatively matches the experimental findings.

There is also evidence for biological manifestations of diffusional pumping [6,9,19,20]. Recent experiments show that water transport is coupled to Na^+ glucose [19] and KCl [6] transport. The negative osmotic reflection coefficient measurements across *Necturus* gallbladder epithelia [6], in particular, have eluded explanation, although

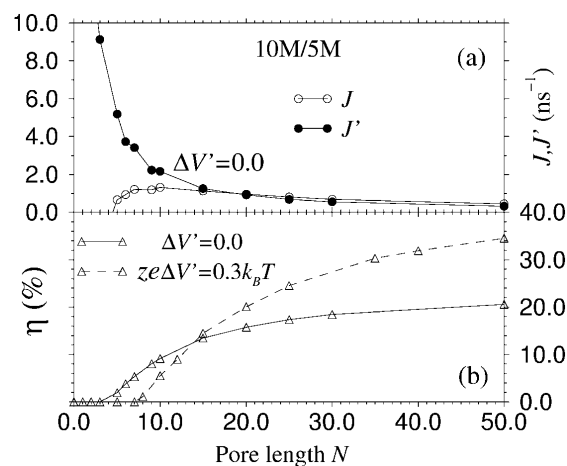


FIG. 3. Dependence of (a) currents and (b) efficiency on pore length $N = L/\ell$ for $ze\Delta V' = 0.0, 0.3k_B T$. The parameters $\{\xi, \xi'\}$ used are the same as those in Fig. 2, except $\chi_L'/\chi_R' = 0.18/0.09$ corresponding to a 10 M/5 M aqueous solution. Although J, J' generally decrease with N , efficiency increases to an asymptotic value.

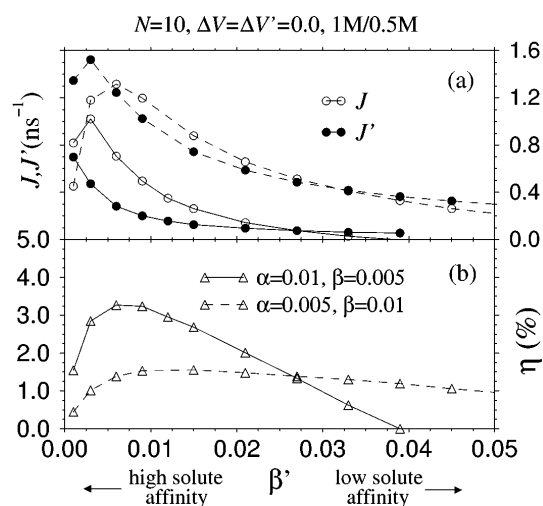


FIG. 4. (a) Currents and (b) efficiencies as functions of B -pore binding ($\sim 1/\beta'$). The solid curves correspond to a slightly A -attracting pore where $\alpha = 0.01$, $\beta = 0.005$. The dashed curves correspond to an A -repelling pore where $\alpha = 0.005$, $\beta = 0.01$.

it is conjectured that separate KCl and water transporters must be near each other in the membrane and coupled [6]. However, we point out that size exclusion dynamics (or extreme solute-solvent coupling) long known to occur in gramicidin channels [4], provides a mechanism for coupled transport. We also describe the conditions under which common membrane channels can mimic symport pumps, conventionally described as more complicated shuttling proteins [2,16,17].

Biological cell membrane channels have sizes that limit diffusional pumping efficiencies, particularly at physiological solute concentrations (Fig. 2). However, the flow rates achievable by simple pores are higher than those of shuttle enzymes and may be a viable mechanism in cellular volume control, or whenever high fluxes are desired. The ubiquity of membrane channels that conduct water [6,19], and are leaky to certain solutes [5–7], suggests our results should be considered for more quantitative interpretations of “negative” osmosis and coupled transport measurements.

More accurate molecular dynamics or Monte Carlo simulations may reveal further details of diffusion pumping. For example, “slippage,” or incomplete coupling processes defined by $\bullet \bullet \rightleftharpoons \bullet \circ$ may occur in wider channels and decrease efficiencies. Similarly, attractive interactions between A - A , A - B , and B - B can affect performance either way. To model two solutes, three species models (e.g., $\tau_i, \tau_i', \tau_i'', \chi + \chi' + \chi'' = 1$) can be used. However, systematic experiments, especially on more controllable artificial membrane systems, are needed to ultimately test the basic energetics outlined.

T. C. was supported by The Wellcome Trust and The National Science Foundation (DMS-98-04780). D.L. acknowledges support from the DFG through Grant No. Lo556/3-1. We have benefited from discussions with E.D. Siggia, T.J. Pedley, A.E. Hill, and S.B. Hladky. We thank T.-H. Her for access to computing facilities.

*Present address: Department of Mathematics, MIT, 77 Massachusetts Avenue, Cambridge, MA 02139.

- [1] R. M. Barrer, *Zeolites and Clay Minerals as Sorbents and Molecular Sieves* (Academic Press, London, 1978).
- [2] B. Alberts *et al.*, *Molecular Biology of the Cell* (Garland, New York, 1994).
- [3] C. Bean, in *Macroscopic Systems and Models*, edited by G. Eisenman, Membranes (Marcel Dekker, New York, 1972).
- [4] O. A. Andersen, *Annu. Rev. Physiol.* **46**, 531 (1984); J. A. Dani and D. G. Levitt, *Biophys. J.* **35**, 501 (1981).
- [5] A. Finkelstein, *Water Movement Through Lipid Bilayers, Pore, and Plasma Membranes* (Wiley-Interscience, New York, 1987).
- [6] T. Zeuthen, *Int. Rev. Cytol.* **160**, 99 (1995); *Proceedings of the Alfred Benzon Symposium 34*, edited by H. H. Ussing *et al.* (Munksgaard, Copenhagen, 1993).
- [7] M. R. Toon and A. K. Solomon, *Biochim. Biophys. Acta* **1063**, 179–190 (1991).
- [8] O. Hahn and D. Woermann, *J. Membr. Sci.* **117**, 197–206 (1996); J. Schink, H. Rottger, and D. Woermann, *J. Colloid Interface Sci.* **171**, 351 (1995).
- [9] W. Y. Gu, W. M. Lai, and V. C. Mow, *J. Biomech.* **30**, 71–78 (1997).
- [10] B. Derrida, *Phys. Rep.* **301**, 65 (1998).
- [11] T. Chou, *Phys. Rev. Lett.* **80**, 85 (1998).
- [12] T. Chou, *J. Chem. Phys.* **110**, 606 (1999).
- [13] S. Tripathi and S. B. Hladky, *Biophys. J.* **74**, 2912 (1998).
- [14] L. Xu, M. G. Sedigh, M. Sahimi, and T. Tsotsis, *Phys. Rev. Lett.* **80**, 3511 (1998).
- [15] V. Russell, C. C. Evans, W. Li, and M. D. Ward, *Science* **276**, 575 (1997).
- [16] D. G. Nicholls and S. J. Ferguson, *Bioenergetics 2* (Academic Press, London, 1992).
- [17] T. L. Hill, *Free Energy Transduction in Biology: The Steady-State Kinetic and Thermodynamic Formalism* (Academic Press, New York, 1977).
- [18] Attractive A -pore affinities are measured by β^{-1} since E_β is large and $\beta \sim \exp(-E_\beta/k_B T)$ is small. As the pore is made less attractive and eventually repulsive, $E_\beta \rightarrow 0$, β increases and saturates to β_0 ; eventually, α decreases as E_α increases [see Fig. 1(b)]. B -pore affinities are similarly defined.
- [19] D. Loo, T. Zeuthen, G. Chandy, and E. M. Wright, *Proc. Natl. Acad. Sci. U.S.A.* **93**, 13 367 (1996).
- [20] A. Su, S. Mager, S. L. Mayo, and H. A. Lester, *Biophys. J.* **70**, 762 (1996).